Research Article

Preparation of NaTaO₃ by Spray Pyrolysis and Evaluation of Apparent Photocatalytic Activity for Hydrogen Production from Water

Hyun Woo Kang, Eun-Jung Kim, and Seung Bin Park

Department of Chemical and Biomolecular Engineering, Korea Advanced Institute of Science and Technology,
373-1 Guseong-dong, Yuseong-gu, Daejeon 305-701, South Korea

Correspondence should be addressed to Seung Bin Park, seungbinpark@kaist.ac.kr

$NaTaO_3$ photocatalyst was prepared by spray pyrolysis process and tested as photocatalyst for water splitting under UV light. Precursor solution was prepared from $NaNO_3$ and $Ta(OC_2H_5)_5$ in nitric acid solution and spray-pyrolyzed in air at between 973 and 1273 K. Considerable enhancement of photocatalytic activity was achieved by loading 0.05~0.2 wt% of NiO on the surface of $NaTaO_3$. The NiO loading was more effective on the $NaTaO_3$ synthesized by spray pyrolysis in comparison with that synthesized by solid-state reaction. The quantum yield (QY) of $NiO/NaTaO_3$ photocatalyst was measured by chemical actinometry using potassium ferrioxalate and compared with the apparent photocatalytic activities (APA) which would be more useful for the purpose of photocatalytic reactor design than the quantum yield. The apparent photocatalytic activity (APA) was defined by the rate of hydrogen production divided by weight of catalyst, volume of reactant mixture, duration of irradiation, and power of UV lamp. The validity of the apparent photocatalytic activity (APA) was discussed based on our results and reported activities of $NaTaO_3$ photocatalyst loaded with or without NiO.

1. INTRODUCTION

Photocatalytic splitting of water by using oxide semiconductors is one of the promising schemes to produce hydrogen from water. Among various metal oxides, $NaTaO_3$ was reported to be one of the most efficient photocatalysts for water decomposition without cocatalyst. The higher potential of the conduction band of $NaTaO_3$ could lead to be more effective to reduce the water to produce H_2 since the tantalates possess conduction bands of Ta5d orbital which are more negative position than titanate (Ti3d) or niobate (Nb4d) [1–3].

Kudo and Kato synthesized $NaTaO_3$ by means of solid-state reaction at high temperature (1420 K) for a long reaction time (10 hours), which resulted in the localized segregation of component and loss of stoichiometry due to evaporation of the constituent components [2, 3].

In this report, a spray pyrolysis was proposed as a way of avoiding problems of solid-state reaction method. The spray pyrolysis process is an aerosol process in which one droplet of precursor solution converts into one particle in short residence time at lower processing temperature than the solid-state reaction process. Because of short residence time and low temperature, the spray pyrolysis method produces powders of high phase-purity and uniformity in composition. Particles produced by the spray pyrolysis are usually spherical and aggregation-free [4, 5].

The quantum yield (QY) has been used to compare the intrinsic activity of photocatalyst. The quantum yield includes the effect of loss of photons scattered or reflected by the photocatalyst itself and absorbed by some impurities or reactants. The number of photons absorbed by photocatalyst has been determined by two methods. One is using the light-flux meter such as a 1815-C (Newport) or a power meter (Advantest, Si diode, TQ8210 or Molectron Power Max 5200). The other is a chemical actinometry method. Potassium ferrioxalate method developed by Parker et al. [6, 7] has been a standard chemical actinometer and used over
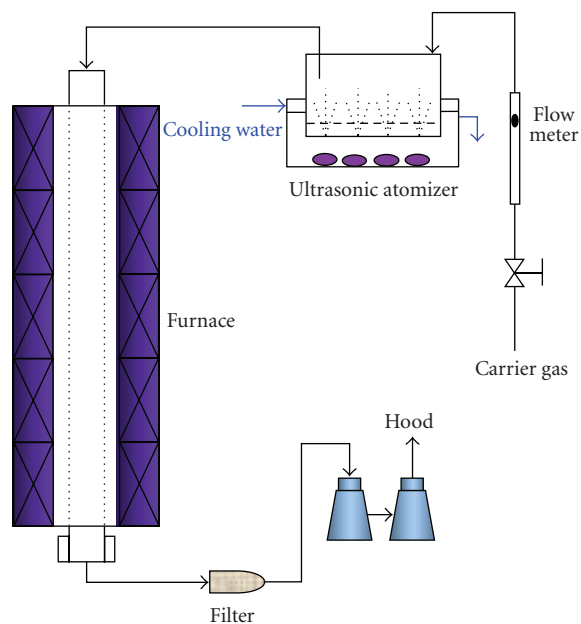
Figure 1: Schematic diagram of spray pyrolysis experimental apparatus.

a broad band of wavelength. However, the exact evaluation of quantum yield for the heterogeneous reaction has not been easy because of the difficulty of measuring the intrinsic number of photons absorbed by photocatalyst. In addition, the quantum yield has been strongly dependent upon the determination methods as well as experimental conditions. It has been frequently encountered that the values of quantum yield have been directly related only to the rate of H_2 evolution, although the experimental conditions such as the amount of catalyst, reactor type, and power of the lamp are quite different.

Therefore, in this report, a new definition of photocatalytic activity was proposed for the purpose of comparing photocatalysts from the reactor design point of view.

2. EXPERIMENT

2.1. Synthesis of photocatalyst

To synthesize the $NaTaO_3$, a spray pyrolysis system which consists of an ultrasonic atomizer, vertical furnace reactor, and particle collector was employed (see Figure 1). A commercial ultrasonic atomizer has four oscillators (Dong-Lim Eng.) with atomizing frequency of 1.7 MHz. The droplets generated by atomizer were transported into vertical furnace reactor by carrier gas (air) at the flow rate of 4~5 L/min and passed through a 0.84 m long and 30 mm i.d. quartz tube. The reactor temperature was controlled at between 973 K and 1273 K. The prepared particles were collected by a thimble filter (28 mm × 100 mm, Toyo Roshi Kaisha Ltd.).

$Ta(OC_2H_5)_5$ (Aldrich, purity 99.98%) and $NaNO_3$ (Junsei, purity 99.5%) were used as precursors. For the preparation of 0.125 M colloid solution, $Ta(OC_2H_5)_5$ was dissolved in distilled water containing excess nitric acid,
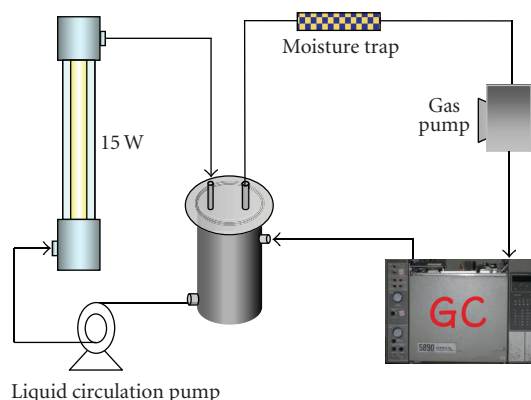

Figure 2: Schematic diagram of experimental apparatus for the measurement of photoactivity for water splitting.

and it was stirred vigorously by magnetic stirrer and heated to 313~353 K or use without heating at 298 K. When the precursor solution became clear or colloid without any precipitates, $NaNO_3$ was added and stirred for dissolution. NiO as cocatalyst was loaded by an impregnation method from aqueous solution of $Ni(NO_3)_2 \cdot 6H_2O$ (Aldrich). $NaTaO_3$ was added to the solution and stirred by magnetic stirrer. Then, water was removed by using a rotary vacuum pump. Finally, the $NiO/NaTaO_3$ powder was calcined at 540 K for 3 hours under air.

2.2. Characterization of photocatalyst

Synthesized powders were identified by X-ray diffraction (Rigaku, D/MAX-RB), and the surface morphology and average particle size of the powders were observed by field-emission SEM (Philips, 533M). The dispersion of NiO on surface of powder was observed by field-emission TEM (FEI, Technai G2 F3 S-Twin). The surface area was determined by BET measurement (Micromeritics, ASAP 2000). A diffuse reflection spectrum was obtained by using a UV-vis-NIR spectrometer (Jasco, Ubest V-570) and was converted from reflection to absorbance by the Kubelka-Munk method.

2.3. Photocatalytic activity measurement

Hydrogen production reactions were carried out in a closed circulation system as shown in Figure 2. The system consisted of reactor, reservoir, and detector (gas chromatograph). The reactor was a donut shape but it had only one Pyrex outer tube without inner quartz tube so that the wall of UV lamp was in direct contact with reactant mixture. Removal of the quartz inner tube reduced the construction cost of this type of slurry reactor. Inner diameter and length of the outer tube were 34 mm and 320 mm, respectively. UV-C lamp of 15 W (SANKYO, Japan) was used as an illuminating source. The wave length of this lamp was predominantly 254 nm (4.9 eV). The photocatalyst powder of 0.06~0.5 g was dispersed in 300~500 mL of distilled pure water or with methanol in the reservoir and stirred with a magnetic stirrer. Before turning on the light, the system was deaerated with N_2 gas for an hour
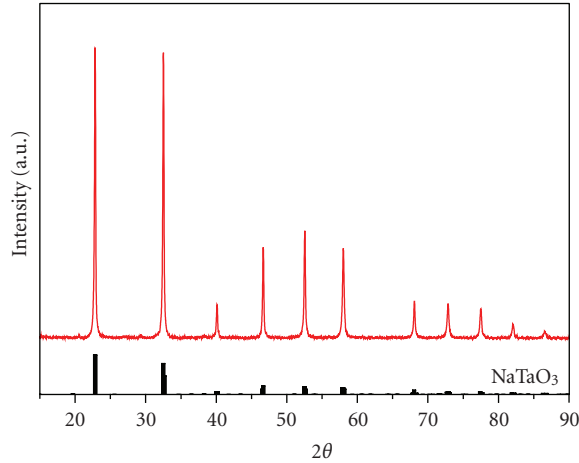
FIGURE 3: XRD pattern of NaTaO₃ powder synthesized by spray pyrolysis (mean residence time = 1.80 seconds, spray pyrolysis temperature = 1173 K, precursor preparation temperature = 333 K, precursor concentration = 0.125 M, carrier gas (air) flow rate = 5 L/min, Na/Ta = 1.00).

and kept at atmospheric pressure. The amount of gas evolved was determined online with gas chromatograph equipped with TCD detector.

2.4. Measurement of quantum yield

The moles of photons absorbed by photocatalyst were measured by a chemical actinometry employing potassium ferrioxalate ($K_3Fe(C_2O_4)_3 \cdot 3H_2O$) synthesized from $K_2C_2O_4 \cdot H_2O$ and $FeCl_3$ to calculate quantum yield. Solution of 0.006 M $K_3Fe(C_2O_4)_3 \cdot 3H_2O$ in 0.06 M H_2SO_4 was prepared and poured into reaction system for irradiation. After 0.1 M $K_3Fe(CN)_6$ was added to sample irradiated, the absorbance was measured by UV-vis spectrophotometer (AIS, DT 1000CE). This work was carried out in a dark room. Finally, the light intensity of an examined light source was determined by[8]

$$I(\text{einsteins/min}) = \frac{A V_2 V_3}{\varepsilon d \varphi_\lambda t V_1}, \quad (1)$$

where A is absorbance, d is length of absorption path, ε is extinction coefficient, φ_λ is QY at wavelength of light used, V_1 is volume of sample, V_2 is volume of actinometer irradiated, V_3 is volume of diluted solution of V_1, and t is irradiated time.

3. RESULTS AND DISCUSSION

The XRD pattern of NaTaO₃ powders synthesized by spray pyrolysis is shown in Figure 3. The main peak appeared at $2\theta = 22.8°$. The XRD pattern confirmed that the homogeneous NaTaO₃ crystal of high crystallinity was synthesized. SEM images of NaTaO₃ were shown in Figure 4. The prepared powders were generally spherical. However, some hollow and shell-like particles are present together. To

TABLE 1: Physical properties of naked sodium tantalates synthesized by spray pyrolysis (NaTaO₃ powder synthesized by spray pyrolysis; mean residence time = 1.80 seconds; spray pyrolysis temperature = 1173 K; precursor preparation temperature = 333 K; precursor concentration = 0.125 M; carrier gas (air) flow rate = 5 L/min; Na/Ta = 1.00).

	Spray pyrolysis
Band gap (eV)	4.0
BET surface area (m²/g)	5.8
Pore volume (cm³/g)	0.019
Average pore size (nm)	8.4

TABLE 2: Effect of NiO loading on photocatalytic activities for water splitting in pure water over NaTaO₃ (NaTaO₃ powder synthesized by spray pyrolysis; mean residence time = 1.80 seconds; spray pyrolysis temperature = 1173 K; precursor preparation temperature = 333 K; precursor concentration = 0.125 M; carrier gas (air) flow rate = 5 L/min; Na/Ta = 1.00; reaction conditions: amount of distilled water, 500 ml; photocatalyst concentration = 1.0 gL⁻¹).

Preparation method	NiO (0.05 wt%) loading	Rate of gas evolution (μmol/hr)	
		H₂	O₂
Spray pyrolysis	X	1.76	—
	O	222	110

optimize the preparation condition, the effect of the precursor preparation temperature on the crystal characteristics was tested. In Figure 5, the optimum precursor preparation temperature was 353 K, and most of samples were prepared at this temperature.

SEM images and XRD patterns of NaTaO₃ powders with variation of spray pyrolysis temperature are shown in Figures 6 and 7, respectively. Based on these two results, the optimum spray pyrolysis temperature was found to be 1173 K. According to the diffuse reflectance spectra of NaTaO₃ powder in Figure 8, the bandgap of NaTaO₃ was estimated to be 4.0 eV. It was determined from the onset of the absorption using the following equation:

$$E_g(\text{eV}) = \frac{1240}{\lambda_g(\text{nm})}. \quad (2)$$

Physical properties such as BET surface area, pore volume, and pore size of NaTaO₃ were summarized in Table 1. The BET surface area was larger by ten times than that of particles synthesized by conventional solid-state reaction.

NiO was loaded on NaTaO₃ synthesized by spray pyrolysis at 1173 K to enhance the photocatalytic activity for water splitting. Figure 9 is TEM image of NiO-loaded NaTaO₃ synthesized by spray pyrolysis. Figure 9(b) is a magnified image of the circle in Figure 9(a). In Figure 9(a), NiO particles (10 nm) were highly dispersed on the surface of NaTaO₃ synthesized by spray pyrolysis.

Table 2 shows the photocatalytic activities for water splitting in pure water over NaTaO₃ with and without NiO.
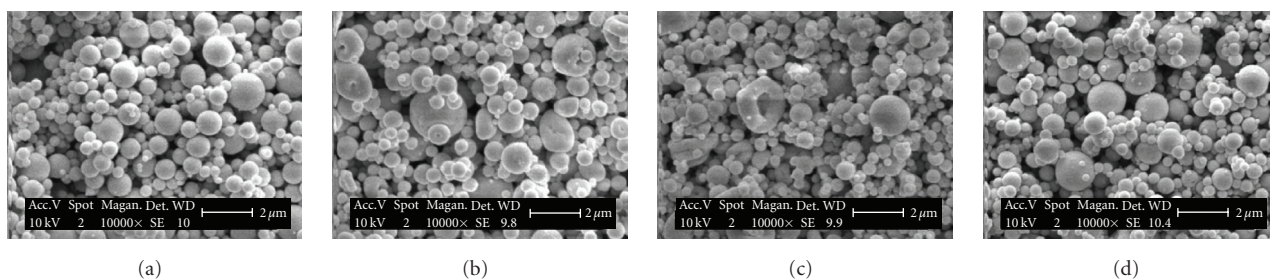
(a)   (b)   (c)   (d)

Figure 4: SEM images of NaTaO$_3$ powders synthesized by spray pyrolysis with variation of precursor preparation temperature: (a) 298 K, (b) 313 K, (c) 333 K, (d) 353 K (mean residence time = 2.25 seconds, spray pyrolysis temperature = 1173 K, precursor concentration = 0.125 M, carrier gas (air) flow rate = 4 L/min, Na/Ta = 1.00).
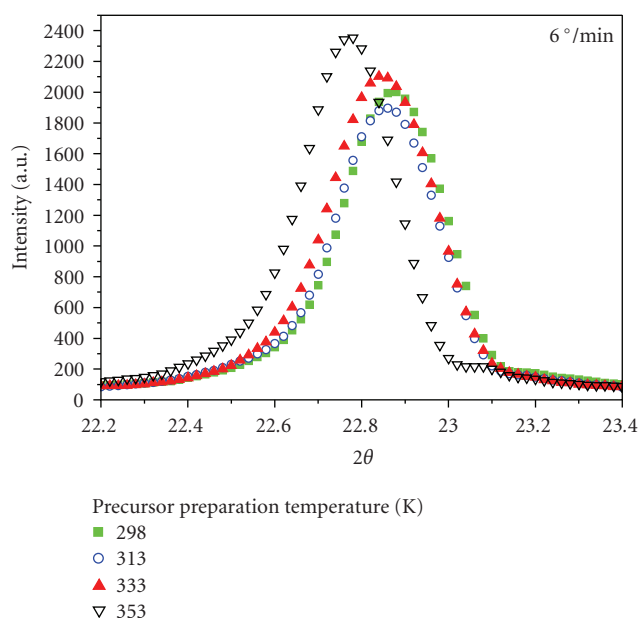

Precursor preparation temperature (K)
- ■ 298
- ○ 313
- ▲ 333
- ▽ 353

Figure 5: XRD patterns of the peak at $2\theta = 22.8°$ for NaTaO$_3$ powder synthesized at several precursor preparation temperatures.

The rate of hydrogen evolution of naked sodium tantalate photocatalysts prepared by spray pyrolysis was 1.76 μmoL/hr while that of NaTaO$_3$ loaded with NiO was dramatically increased to 222 μmoL/hr. The activity enhancement factor by NiO/NaTaO$_3$ synthesized in the present work was much larger than that of NiO/NaTaO$_3$ synthesized by means of the conventional solid-state reaction [2, 3]. Figure 10 shows that the cumulative amount of gas evolution increases almost constantly with irradiation time and the ratio of hydrogen and oxygen is maintained at 2.

In order to determine the optimum loading of photocatalyst, effect of photocatalyst loading (NiO (0.2 wt%)/NaTaO$_3$) on the rate of H$_2$ evolution and quantum yield was tested, and results are shown in Figure 11. The optimum loading was found to be around 0.4 g/L.

The quantum yield (QY), which is defined by (3), has been used to evaluate the activity of photocatalyst over a broad band of wavelength:

$$QY = \frac{\text{moles of product formed}}{\text{moles of photons absorbed}}$$
$$= \frac{2 \times \text{moles of H}_2}{\text{moles of photons absorbed by photocatalyst}}. \quad (3)$$

In order to design an optimum photocatalytic reactor system, consumption of photocatalyst, electric power, volume of slurry reactor, and duration of reaction should be minimized, if catalysts with high-quantum yield were available.

To evaluate photocatalysts for the purpose of optimal design of photocatalytic reactor, the apparent photocatalyst activity (APA) is proposed as

$$APA = \frac{\text{moles of H}_2 \text{ evolution}}{(X)(Y)(Z)(W)}, \quad (4)$$

where X = weight of catalyst, Y = volume of reactant, Z = duration of reaction and W = power of lamp.

This definition is more useful for designing a photocatalytic reactor than the quantum yield. The calculated values of the apparent photocatalytic activity from literature were summarized in Table 3, along with the reported values of quantum yield. For comparison, the values of APA and quantum yield of the current work were summarized in Table 4. It should be noted that the reactors, types of lamps, and measurement methods of photon intensity were different in those tables.

Figure 12 is a plot of APA versus quantum yield for data summarized in Tables 3 and 4. It is clear that the high-quantum yield is not always preferable criterion from the reactor design point of view. For example, the rate of H$_2$ evolution reported by Abe et al. [11] is 220 μmoL/hr and that of present study by using NaTaO$_3$ is 237.5 μmoL/hr, and the quantum yields are also very similar to each other. However, the APA for the catalyst of Abe et al. [11] is 2.7 μmoL/g·L·hr·W whereas that of the present work is 439.8 μmoL/g·L·hr·W, although the rate of hydrogen evolution is very similar.

Figure 13 is a plot of apparent photocatalytic activity of current work and published results. The APA of current
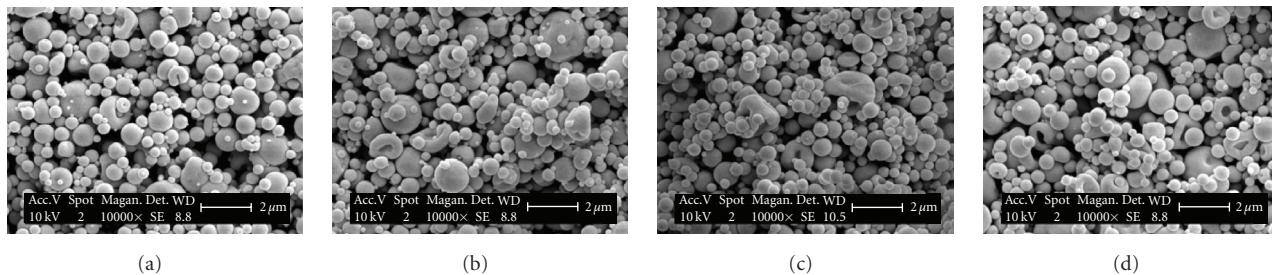
(a)   (b)   (c)   (d)

FIGURE 6: SEM images of NaTaO$_3$ powders synthesized by spray pyrolysis with variation of spray pyrolysis temperature: (a) 973 K, (b) 1073 K, (c) 1173 K, (d) 1273 K (mean residence time = 1.80 seconds, precursor preparation temperature = 333 K, precursor concentration = 0.125 M, carrier gas (air) flow rate = 5 L/min, Na/Ta = 1.00).

TABLE 3: Quantum yield (QY) obtained by (1) and apparent photocatalytic activity (APA) obtained by (2) of several semiconductor photocatalysts for water splitting.

Photocatalyst	Reactor	Reactant volume (L)	H$_2$ (μmol/hr)	Actinometer [light used]	Apparent photocatalytic activity	Ref.
	Lamp	Catalyst (g)	QY (%)		(μmole/g·L·hr·W)	
NiO/TiO$_2$	Pyrex cylinder	0.3	600	Potassium ferrioxalate [−]	14.29	Lee et al. (2001) [9]
	700 W High pressure Hg lamp	0.2	12.0			
NiO$_x$/RbTaWO$_6$	Quartz reaction cell	0.07	69.7	Spectra radiometer [313 nm]	3.32	Ikeda et al. (2004) [10]
	1 kW superpressure Hg lamp	0.3	1.5			
Pt/TiO$_2$-A1 and TiO$_2$-R2	Inner irradiation type reactor	0.5	220	Thermopile power meter [350 nm]	2.75	Abe et al. (2005) [11]
	400 W high pressure Hg lamp	0.4	4.0			
NiO$_x$/Ba$_2$In$_2$O$_5$/ In$_2$O$_3$:Cr	Inner irradiation quartz cell	0.5	29.3	−[320 nm]	0.40	Wang et al. (2005) [12]
	400 W high pressure Hg lamp	0.37	4.2			
Sr$_2$Nb$_2$O$_7$	Inner irradiation quartz cell	0.35	402	Ferrioxalate Fe(C$_2$O$_4$)$_3^{3-}$ [< 300 nm]	2.55	Kim et al. (1999) [13]
	450 W high pressure Hg lamp	1	23			
Pt/(AgIn)$_{0.22}$ Zn$_{1.56}$S$_2$	Side window Pyrex cell	0.3	944	Photodiode [420 nm]	34.96	Tsuji et al. (2004) [14]
	300 W Xe lamp	0.3	20			
NiO$_y$/ In$_{0.9}$Ni$_{0.1}$TaO$_4$	Pyrex glass cell	0.25	16.6	−[402 nm]	0.44	Zou et al. (2001) [15]
	300 W Xe lamp	0.5	0.67			
NiO/NaTaO$_3$	Inner irradiation quartz cell	0.35	2180	Ammonium ferrioxalate [270 nm]	15.57	Kato and Kudo (1999) [2]
	400 W high pressure Hg lamp	1	28			
NiO/NaTaO$_3$:La	Inner irradiation quartz cell	0.39	15000	Ammonium ferrioxalate [270 nm]	96.15	Kudo and Kato (2000) [16]
	400 W high pressure Hg lamp	1	50			

TABLE 4: Quantum yield (QY) obtained by (1) and apparent photocatalytic activity (APA) obtained by (2) of photocatalysts in the present study for water splitting (reactor, Pyrex cylinder; lamp, 15 W UV-C lamp; actinometer, potassium ferrioxalate).

Photocatalyst	Precursor preparation temperature (K)	Mean residence time (sec)	Reactant volume (L)	H_2 (μmol/hr)	Apparent photocatalytic activity (μmole/g·L·hr·W)
	Spray pyrolysis temperature (K)	Sacrificial agent (methanol 20 vol%)	Catalyst (g)	QY (%)	
NiO(0.05 wt%)/ NaTaO$_3$	333	1.80	0.5	462.5	**123.3**
	1173	X	0.5	**6.5**	
NaTaO$_3$	333	1.80	0.5	0.27	**0.07**
	973	X	0.5	$\mathbf{3.8 \times 10^{-3}}$	
NaTaO$_3$	333	1.80	0.5	1.25	**0.33**
	1073	X	0.5	$\mathbf{1.8 \times 10^{-2}}$	
NaTaO$_3$	333	1.80	0.5	3.31	**0.88**
	1173	X	0.5	$\mathbf{4.6 \times 10^{-2}}$	
NaTaO$_3$	333	1.80	0.5	0.81	**0.22**
	1273	X	0.5	$\mathbf{1.1 \times 10^{-2}}$	
NaTaO$_3$	298	2.25	0.3	107.5	**199.1**
	1173	O	0.12	**1.5**	
NaTaO$_3$	313	2.25	0.3	300.0	**555.6**
	1173	O	0.12	**4.2**	
NaTaO$_3$	333	2.25	0.3	237.5	**439.8**
	1173	O	0.12	**3.3**	
NaTaO$_3$	353	2.25	0.3	2150.0	**3981.5**
	1173	O	0.12	**30.1**	
NiO(0.2 wt%)/ NaTaO$_3$	353	2.25	0.3	1625.0	**6018.5**
	1173	O	0.06	**22.8**	
NiO(0.2 wt%)/ NaTaO$_3$	353	2.25	0.3	3150.0	**5833.3**
	1173	O	0.12	**44.1**	
NiO(0.2 wt%)/ NaTaO$_3$	353	2.25	0.3	3637.5	**4490.7**
	1173	O	0.18	**50.9**	
NiO(0.2 wt%)/ NaTaO$_3$	353	2.25	0.3	3212.5	**2379.6**
	1173	O	0.30	**45.0**	

work is almost equal or slightly better than the highest APA reported by Kudo and Kato [16] although the quantum yield of the current work is lower than that of Kudo and Kato's result.

However, the purpose of this paper is not to claim that we prepared superior photocatalyst, but to claim that both quantum yield and apparent photocatalytic activity are equally important when comparing the performance of photocatalyst for water splitting.

4. CONCLUSION

(1) NaTaO$_3$ photocatalyst was synthesized by means of spray pyrolysis in relatively mild experimental conditions: 973~1273 K of reaction temperature and 1.80~2.25 seconds of residence time. The reaction temperature and duration of reaction are 1420 K and 10 hours, respectively, when NaTaO$_3$ was prepared by the conventional solid-state reaction

(2) To enhance the photocatalytic activity for water splitting, 0.05~0.2 wt% of NiO was loaded on the surface of NaTaO$_3$ powder synthesized by spray pyrolysis, which resulted in a considerable increase of photocatalytic activity in comparison with that of NaTaO$_3$ powder synthesized by means of conventional solid-state reaction.

(3) A new definition of photocatalytic activity was proposed from the reactor design point of view and named as apparent photocatalytic activity (APA), which is defined by the rate of hydrogen production divided by amount of catalyst, volume of reactant, duration of reaction, and power of lamp irradiated.

(4) Quantum yield is an important criterion to screen photocatalyst. However, the high-quantum yield is not always preferable for designing an economically feasible photocatalytic reactor system. Small size reactor, small amount of photocatalyst, short reaction time, and low consumption of power are also important for economically competitive
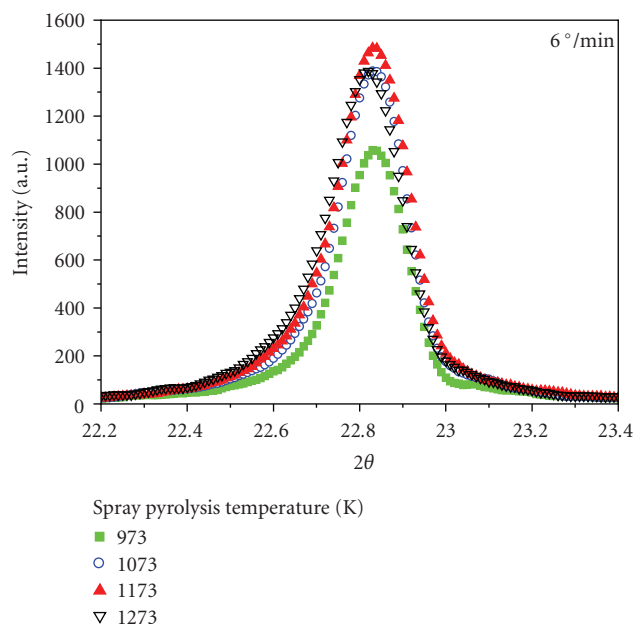
FIGURE 7: XRD patterns of the peak at $2\theta = 22.8°$ for NaTaO₃ powder synthesized at several spray pyrolysis temperatures.
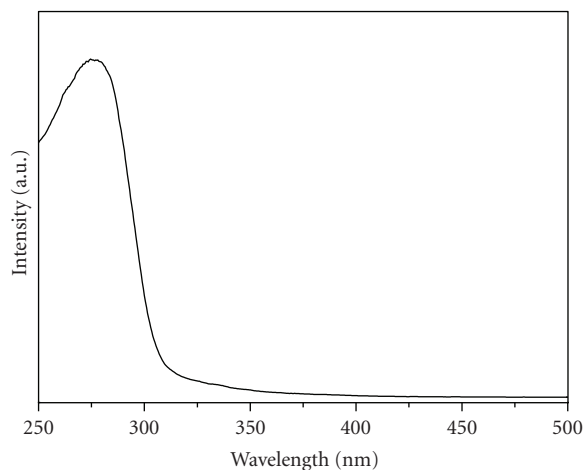

FIGURE 8: Diffuse reflectance spectra of the NaTaO₃ powder synthesized by spray pyrolysis (mean residence time = 1.80 seconds, spray pyrolysis temperature = 1173 K, precursor preparation temperature = 333 K, precursor concentration = 0.125 M, carrier gas (air) flow rate = 5 L/min, Na/Ta = 1.00).

production of hydrogen. Therefore, it is strongly recommended to report the apparent photocatalytic activity along with quantum yield when improvement of photocatalytic activity is to be reported.

(5) In this report, only the case of slurry reactor was discussed. If the type of photocatalytic reactor is a flat-surface reactor, the apparent photocatalytic activity would be reported in terms of unit surface area in place of the volume
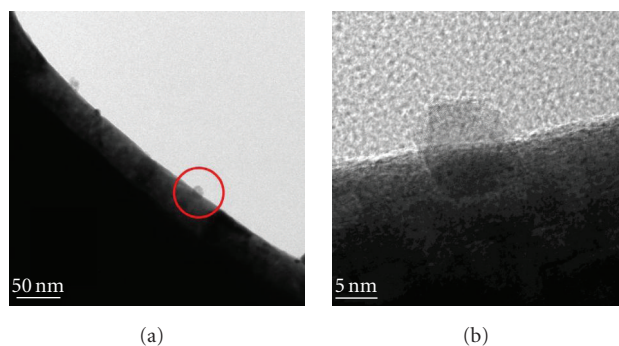

FIGURE 9: TEM images of NiO(0.05 wt%)/NaTaO₃ synthesized by spray pyrolysis; (b) is high magnification of circled location in the (a).
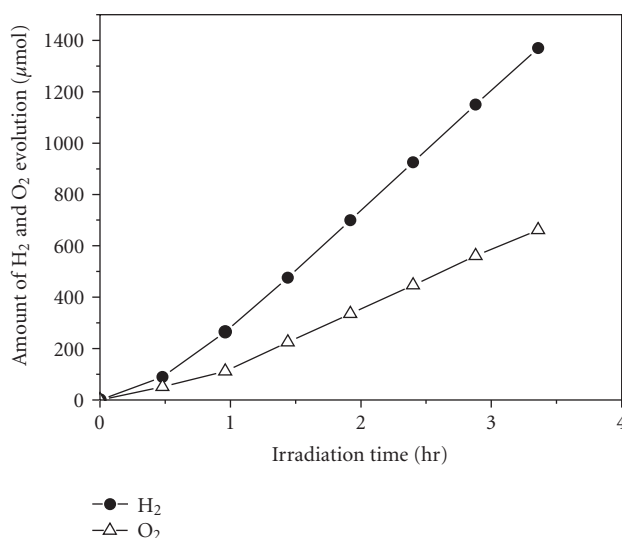

FIGURE 10: Cumulative amount of gas evolution with irradiation time in pure water over NiO(0.05 wt%)/NaTaO₃. (NaTaO₃ powder synthesized by spray pyrolysis, mean residence time = 1.80 seconds, spray pyrolysis temperature = 1173 K, precursor preparation temperature = 333 K, precursor concentration = 0.125 M, carrier gas (air) flow rate = 5 L/min, Na/Ta = 1.00. Reaction conditions: photocatalyst type, NiO(0.05 wt%)/NaTaO₃, amount of distilled water, 500 mL, photocatalyst concentration = 1.0 gL⁻¹).
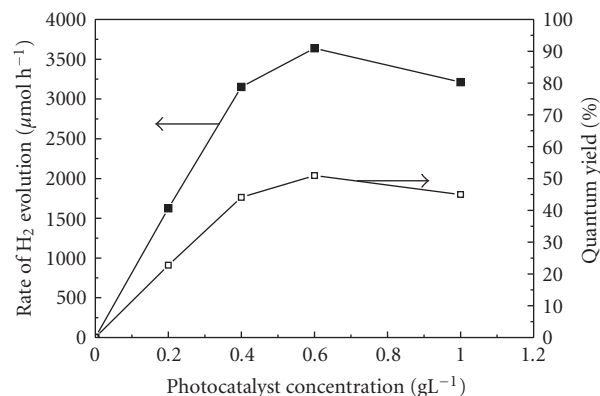

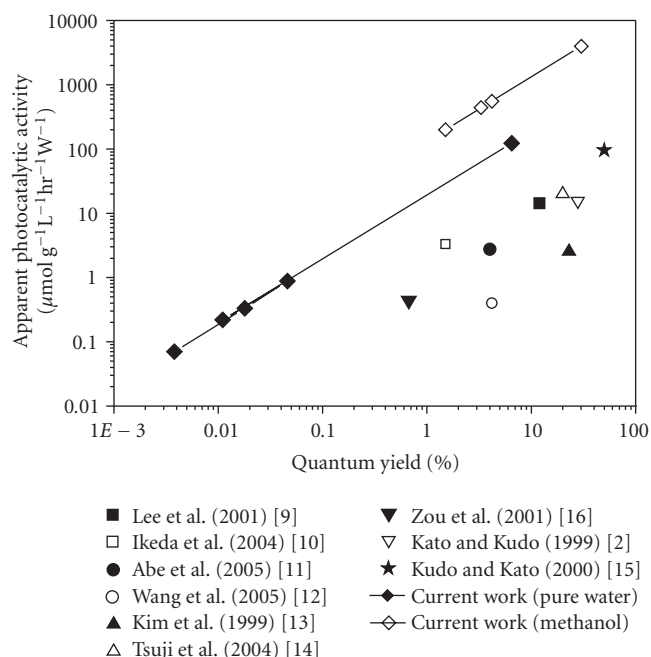FIGURE 11: Determination of optimum amount of photocatalyst loading.

FIGURE 12: Evaluation of photocatalyst performance based on quantum yield and apparent photocatalytic activity.

a: Lee et al. (2001) [9]   f: Tsuji et al. (2004) [14]
b: Ikeda et al. (2004) [10]   g: Zou et al. (2001) [16]
c: Abe et al. (2005) [11]   h: Kato and Kudo (1999) [2]
d: Wang et al. (2005) [12]   i: Kudo and Kato (2000) [15]
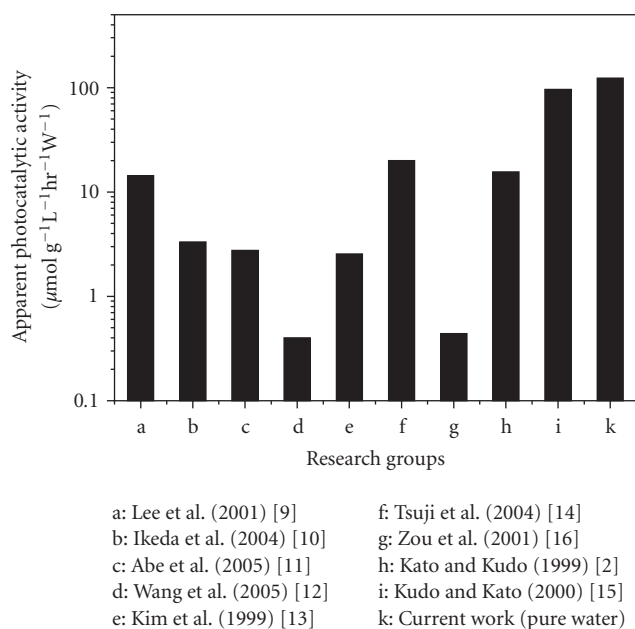e: Kim et al. (1999) [13]   k: Current work (pure water)

FIGURE 13: Comparison of apparent photocatalytic activity of current work with that of published results.

of reactor, because the goal of reactor design is to maximize the hydrogen evolution per unit surface area.

REFERENCES

[1] A. Kudo, "Development of photocatalyst materials for water splitting," *International Journal of Hydrogen Energy*, vol. 31, no. 2, pp. 197–202, 2006.

[2] H. Kato and A. Kudo, "Highly efficient decomposition of pure water into H_2 and O_2 over $NaTaO_3$ photocatalysts," *Catalysis Letters*, vol. 58, no. 2-3, pp. 153–155, 1999.

[3] H. Kato and A. Kudo, "Photocatalytic water splitting into H_2 and O_2 over various tantalate photocatalysts," *Catalysis Today*, vol. 78, no. 1–4, pp. 561–569, 2003.

[4] A. Gurav, T. Kodas, T. Pluym, and Y. Xiong, "Aerosol processing of materials," *Aerosol Science and Technology*, vol. 19, no. 4, pp. 411–452, 1993.

[5] G. L. Messing, S.-C. Zhang, and G. V. Jayanthi, "Ceramic powder synthesis by spray pyrolysis," *Journal of the American Ceramic Society*, vol. 76, no. 11, pp. 2707–2726, 1993.

[6] C. A. Parker, "A new sensitive chemical actinometer. I. Some trials with potassium ferrioxalate," *Proceeding of the Royal Society of London. Series A*, vol. 220, no. 1140, pp. 104–116, 1953.

[7] C. G. Hatchard and C. A. Parker, "A new sensitive chemical actinometer. II. Potassium ferrioxalate as a standard chemical actinometer," *Proceeding of the Royal Society of London. Series A*, vol. 235, no. 1203, pp. 518–536, 1956.

[8] S. L. Murov, G. L. Hug, and I. Carmichael, *Handbook of Photochemistry*, Marcel Dekker, New York, NY, USA, 2nd edition, 1993.

[9] S. G. Lee, S. Lee, and H.-I. Lee, "Photocatalytic production of hydrogen from aqueous solution containing CN^- as a hole scavenger," *Applied Catalysis A*, vol. 207, no. 1-2, pp. 173–181, 2001.

[10] S. Ikeda, T. Itani, K. Nango, and M. Matsumura, "Overall water splitting on tungsten-based photocatalysts with defect pyrochlore structure," *Catalysis Letters*, vol. 98, no. 4, pp. 229–233, 2004.

[11] R. Abe, K. Sayama, and H. Sugihara, "Development of new photocatalytic water splitting into H_2 and O_2 using two different semiconductor photocatalysts and a shuttle redox mediator IO^{3-}/I^-," *Journal of Physical Chemistry B*, vol. 109, no. 33, pp. 16052–16061, 2005.

[12] D. Wang, Z. Zou, and J. Ye, "Photocatalytic water splitting with the Cr-doped $Ba_2In_2O_5/In_2O_3$ composite oxide semiconductors," *Chemistry of Materials*, vol. 17, no. 12, pp. 3255–3261, 2005.

[13] H. G. Kim, D. W. Hwang, J. Kim, Y. G. Kim, and J. S. Lee, "Highly donor-doped (110) layered perovskite materials as novel photocatalysts for overall water splitting," *Chemical Communications*, no. 12, pp. 1077–1078, 1999.

[14] I. Tsuji, H. Kato, H. Kobayashi, and A. Kudo, "Photocatalytic H_2 evolution reaction from aqueous solutions over band structure-controlled $(AgIn)_xZn_{2(1-x)}S_2$ solid solution photocatalysts with visible-light response and their surface nanostructures," *Journal of the American Chemical Society*, vol. 126, no. 41, pp. 13406–13413, 2004.

[15] Z. Zou, J. Ye, K. Sayama, and H. Arakawa, "Direct splitting of water under visible light irradiation with an oxide semiconductor photocatalyst," *Letters to Nature*, vol. 414, pp. 625–627, 2001.

[16] A. Kudo and H. Kato, "Effect of lanthanide-doping into $NaTaO_3$ photocatalysts for efficient water splitting," *Chemical Physics Letters*, vol. 331, no. 5-6, pp. 373–377, 2000.